Conceptual studies on optical diagnostic systems for plasma control on DEMO

W. Gonzalez[a], W. Biel[a], Ph. Mertens[a], M. Tokar[a], O. Marchuk[a], Ch. Linsmeier[a],

[a] *Forschungszentrum Jülich GmbH, Institut für Energie- und Klimaforschung - Plasmaphysik, 52425 Jülich, Germany*

The roadmap to the realization of fusion energy describes a path towards the development of a DEMO tokamak reactor, which is expected to provide electricity into the grid by the mid of the century [1]. The DEMO diagnostic and control (D&C) system must provide measurements with high reliability and accuracy, not only constrained by space restrictions in the blanket, but also by adverse effects induced by neutron, gamma radiation and particle fluxes. In view of the concept development for DEMO control, an initial selection of suitable diagnostics has been obtained [2]. This initial group of diagnostic consists of 6 methods: Microwave diagnostics, thermo-current measurements, magnetic diagnostics, neutron/gamma diagnostics, IR interferometry/polarimetry, and a variety of spectroscopic and radiation measurement systems. A key aspect for the implementation, performance and lifetime assessment of these systems on DEMO, is mainly attributable to their location, that must be well protected, and meet their own set of specific requirements. With this in mind, sightline analysis, space consumption and the evaluation of optical systems are the main assessment tools to obtain a high level of integration, reliability and robustness of all this instrumentation; essential features in future commercial fusion power nuclear plants. In this paper we concentrate on spectroscopic and radiation measurement systems that require sightlines over a large range of plasma regions and inner reactor surfaces. Moreover, this paper outlines the main results and strategies adopted in this early stage of DEMO conceptual design to assess the feasibility of this initial set of diagnostic methods based on sightlines and the integration of these needed for DEMO D&C.

DEMO, plasma diagnostic, plasma control, spectroscopy, radiation measurements

1. Introduction

Unlike current D&C systems developed for fusion experiments, a DEMO D&C system has to ensure machine operation in compliance with nuclear safety requirements and high plant availability [3]. In this regard, all R&D activities for the ITER D&C constitute an invaluable source of experience and information about the last technological and scientific developments. This paper focus on the study of 14 suitable diagnostic methods based on ITER mature technologies for spectroscopy and radiation measurement systems on DEMO. Sightline configurations and common technical aspects are discussed, in line with the application of a system engineering approach; considered to be essential from the early DEMO concept design stage [4].

The paper is organized as follows: In the next section, concepts such as (i) sightline and deviation angle constrains are introduced; (ii) secondly, the basic criteria for first optical component locations are discussed and the optical approach exposed, to conclude with the (iii) sightline configuration proposed for 14 D&C systems and its integration on DEMO. Finally, major results and conclusions are reported, aimed to open new discussions addressed to the DEMO conceptual design.

2. Sightlines and deviation angles

Considering the subset of diagnostic systems for DEMO, see table (2) [2], the development of a robust and reliable D&C system, which optimizes space utilization, will entail a high level of integration between all systems. In this context, spectroscopy and radiation measurements diagnostic systems have an essential role for basic control and machine protection by requiring optical components to channel the electromagnetic radiation through the structures that provide the vacuum and magnetic confinement to the plasma. Such channels “ducts” can be classified according to their plane of orientation as: Poloidal, toroidal or oblique, and more specifically, by their mechanical features such as: Number of openings, and diameter (ρ) (in a range from 10 to 30 mm), optical sightline configuration and length (L), see Figure 1.

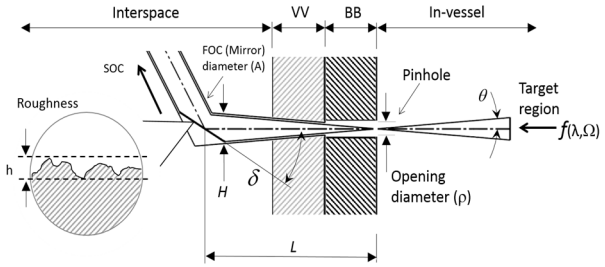

Figure 1: Sightline description and optical approach. Abbreviations: (VV) Vacuum vessel, (BB) Breeding blanket, (FOC) First optical component, (SOC) Secondary optical component.

Optics sightline configurations are mainly characterized by the plasma region under observation (target region), wavelength (λ) of the signal to be measured, angular field (θ) and solid angle (Ω). In addition, the use of mirrors involves deviations (φ) and grazing angles (δ), that can be determined by the equation $\varphi = 2 * \delta$, where φ is the angle between the incident vector $\vec{u}$ and reflected vector $\vec{v}$, see Figure 2 ; creating labyrinth paths to prevent interferences with the host structure and to avoid adverse effects caused by strong

Author email: winder.gonzalez@gmail.com

heat, radiation and particle fluxes, in particular, the damage induced by high neutron fluences on detectors [3]. At the same time, these deviations can lead to substantial signal intensity losses.

In order to address these issues, this work carries out the study of first and secondary optical component locations on 14 different D&C systems for spectroscopy and radiation measurements in flat-top equilibria scenario [4], integrated in 5 equatorial (EQ) and 2 vertical (VP) ports, with a common redundancy equal to 2, except for diagnostic on limiters, which redundancy is equal to 4, considering their operational limits within an optical conservative approach.

1. First optical component (FOC) locations and pinhole optical approach

FOC is the term used to describe the devices in direct observation of the plasma; among the main tentative list of diagnostic methods showed in table (2) for DEMO, we can point out the use of (i) filter foils in methods S1 and S2, (ii) mirrors in methods from S3 to S10 and (iii) radiation detectors (Bolometers) in methods from S11 to S14. FOC's performance and their lifetime are strictly linked to the negative effects, induced by the exposition and proximity to the plasma, such as sputtering and particle deposition; encouraging an extended use of straight ducts penetrations, with large (L/ρ) ratio, integrated within equatorial and vertical port plugs to protect optical components; requiring in cases of X-ray and VUV measurements, locations outside the vacuum vessel region, within vacuum extensions.

Whereas the filter foils and bolometers could operate at locations distant from the plasma, more often the mirrors locations are confined to areas near to the Breeding blanket (BB), where the requirements imposed by the target geometry region and the limited accessibility are satisfied. In this respect, it is essential to estimate the maximum allowed surface roughness (h_{max}) on mirrors, to guarantee a high specular reflection throughout its lifetime. To this end, mirror optical flatness could be estimated by the equation $h_{max} \leq \lambda/10 * \sin\delta$ [6], considering the wavelength range and grazing angle δ, within a constructive phase difference of $\Delta\phi \leq 2\pi/5$, see table (2). In addition to the aforementioned concept, the implementation of the pinhole principle in ducts is under consideration to prevent the FOC's degradation; since small openings, can limit the entry of high energy atoms into the diagnostic ducts, avoiding potential impacts on FOC's [8].

2. Diagnostic systems and sightline configuration proposal

To address an integral conceptual study of these systems, the first consideration has been the diagnostic method classification by signal wavelength range to be measured and their optics conditions as function of the interaction with FOC's, followed by the evaluation of the requirements imposed by the target region and the geometry of the host ports, bearing in mind the space limitation on the breading blanket (BB) to ensure the Tritium Breeding ratio (TBR>1) and the restrictions imposed by the expected level of neutron fluence at equatorial (EP) and vertical (VP) ports on DEMO [7].

Basic sightline requirements by target region are described as follow: (i) Plasma core diagnostic is represented by systems S1, S2, S3 and S10, composed by sightlines contained within the EP, going through the plasma centre in poloidal orientation and tomography approach; plasma core diagnostics are aimed at the control of high-Z impurity accumulation, MHD control and core radiation power measurements. (ii) Plasma edge diagnostic is represented by systems S4 and S12, composed by sightlines contained within the EP and VP, monitoring the upper edge high field side (U-HFS), upper edge low field side (U-LFS) and lower edge low field side (L-LFS) in poloidal orientation. Edge diagnostic systems are intended to provide measurements of concentrations of all relevant impurity species (from He to W) [2] and the control of plasma edge radiation power. (iii) Divertor diagnostic is represented by systems S5, S6, S8 and S14, composed by tangential (spectroscopy) and oblique (thermography) sightlines contained within the EP, looking along the divertor target allowing for some spatial resolution, in oblique orientation. Main purposes of this group of diagnostic are the control of plasma detachment, temperature and radiation power on divertor target region. (iv) Limiter diagnostics are represented by systems S7 and S9; these are composed by tangential (spectroscopy) and oblique (thermography) sightlines contained within the EP, monitoring 4 limiters locations (Upper-plane, Mid-plan, lower-plane and inner FW) in poloidal, toroidal and oblique orientation. Limiter diagnostic function is the Edge localized modes (ELM) detection and control of the plasma flow to limiters. (v) X-point diagnostic is represented by system S13, composed by sightlines looking into the nominal x-point, more specifically, about +/- 45 cm above and below the nominal x-point, in poloidal orientation, for plasma radiation power control near the x-point.

Sightline configurations for each diagnostic system shown in table (2), have been developed through the establishment of sightlines between key points from their respective target regions to feasible FOC locations, represented by vectors $\vec{u}$ and $\vec{v}$, see Figure 2; keeping the following criteria under consideration: (i) Diagnostic sightlines should be completely contained within EP and VP plugs, avoiding interferences with other structures; (ii) the amount of openings must be limited, encouraging the integration between sightlines and different diagnostic methods, if possible; (iii) unnecessary sightline intersections must be avoided, preserving consistency with the plane of orientation and suitable deviation angles φ for secondary optical component (SOC) locations; (iv) in order to restrain the erosion under the limit of 1nm/fpy; sightlines with (L/ρ) > 70 for VUV spectroscopy, (L/ρ) > 50 for VIS spectroscopy and (L/ρ) > 40 for IR diagnostics are mandatory, in view of the results obtained by M.Tokar in [8], and the equation 1, used as an approximation for the erosion rate estimation, at the distance L [m], with a working gas density $n_g=3*10^{19}$ [m^3] in the duct and an opening diameter ρ = 30 mm.

$$h_{[nm,fpy]} = 3000e^{-4.8*L} \quad (1)$$

As a result of this phase, sightlines, FOC and SOC locations have been established, allowing the estimation of the (L/ρ) ratio by wavelength range, see table (1), the minimum $(L/\rho)_{min}$ ratio and grazing angle (δ_{min}) by system, in accordance with the above mentioned criteria, see table (2).

Wavelength range	h_{max} [nm]	h_{max} [nm]/fpy	L [m]	(L/ρ) , ρ = 30 [mm]
VUV	4,3	0,86	1,07	57
VIS	40	8	1,24	41
IR	300	60	1,15	27
ECE*	78	15,6	1,09	37

Table 1: Minimum (L/ρ) ratio by wavelength range. (*) Forward-beamed continuum emission in the near IR range is expected to be dominated by synchrotron emission from fast electrons [9].

For instance, in case of the installation of mirrors to provide neutron shielding to bolometers, Figure 2 shows the deviation angle φ and minimum grazing angle δ_{min}=11° for S12 at EP. Finally, a proposal for the distribution of all systems (including redundancy) on 5 sectors of DEMO has been elaborated and shown in Figure 4.

3. Results

Table (2), summarize the subset of diagnostic systems based on spectroscopy and radiation measurements for DEMO, organized by wavelength ranges from S1 to S14 and described by number of EP and VP sightlines. Sightline analysis and visualization have been carried out in Python, where FOC's and SOC's locations have been evaluated and stablished for each system. As a result, minimum grazing angles δ_{min} have been estimated, aimed to identify the critical sightline condition for mirror reflectance (R) and mirror maximum roughness allowed h_{max}. In the same way, the minimum $(L/\rho)_{min}$ ratio and the expected surface roughness (h_f) after 5 fpy of operation have been estimated, considering an opening diameter ρ = 30 mm, in all cases.

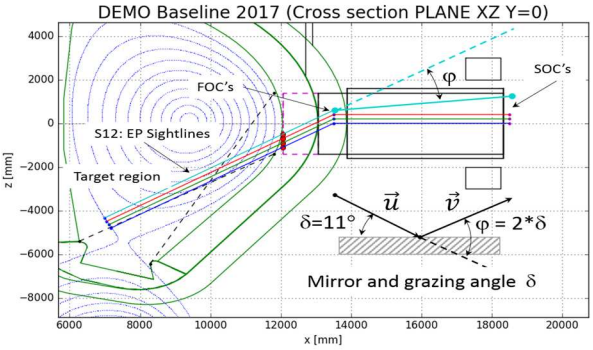

Figure 2: EP-S12 diagnostic sightlines and minimum grazing angle δ_{min} estimation to prevent interferences with the EP structure.

All these systems have been assessed by focusing on the sightline integration with equal orientation plane, for this purpose, three composed diagnostic modules (CDM) have been conceptualized and designed, see Figure 3. CDMs are described as follows: CDM_A: This module contains systems with poloidal orientation; occupied different parallel XZ planes and sightlines distributed in EP and VP; hosted systems are reported in Figure 3. CDM_B: This module contains systems with oblique orientation and equal target region (divertor region for S5, S6 and S14); this module shows a limited capacity of integration with other systems, because of the sightlines passing throughout the entire oblique EP space. Although all sightlines are contained within the EP, looking into the same target region, sightline intersections are avoided by a shift in Z coordinate at FOC locations. CDM_C: This module contains systems with oblique and toroidal orientation, where systems S7, S8 (Outer divertor) and S9 are hosted and particularly S8 sightlines does not cross the plasma core. Similarly, space limitations and sightline configurations of these systems, reduce the possibility of a hypothetical integration of this module with the CDM_B, for example; nevertheless, further analysis is needed to investigate the feasibility at a greater level of integration.

Table 2: D&C systems based on spectroscopy and radiation measurements selected for DEMO; sightline configuration and summary of results by system are reported. Symbol (-) indicate no geometrical limits or no sightline to the extraction of the beam through the host port. Symbol (*) indicate that EP δ_{min} = 8° is assumed based on the proposal VUV spectrometer system for DEMO [2]. Symbol (**) indicate that at this distance sputtering erosion is not expected. (1) ECE oblique sightline is not foreseen in this study [10]. (2) The installation of mirrors to provide neutron shielding to bolometers is under consideration.

Wavelength range	System # and method		Target region	EP Sightlines	VP Sightlines	First optical component (FOC)	EP (δ) min [Deg.]	h_{max} [nm]	$(L/\rho)_{min}$, ρ = 30 [mm]	h_f [nm]: n_g = 3E19 [m^{-3}], (L/ρ)min, at @5 fpy	Integration CDM_(EP)	Integration CDM_(VP)
[0.01 - 10] nm	S1	HR X-ray Spectroscopy	Core	3	-	(Be) Filter foil	-	n/a			CDM _A (EP9 & EP12)	n/a
	S2	X-ray Intensity	Core	13	12		-					CDM _A (VP9 & VP12)
[6 - 125] nm	S3	VUV Spectroscopy	Core	4	-	(Pt, Au) Mirror	8*	4,3	101	**	CDM _A (EP9 & EP12)	n/a
	S4	VUV Spectroscopy	Edge	4	8		13,5	2,6	84	0,05		CDM _A (VP9 & VP12)
	S5	VUV Spectroscopy	Divertor	12	-		13	2,7	71	0,36	CDM _B (EP10)	n/a
[400 - 700] nm	S6	VIS Spectroscopy	Divertor	12	-	(Rh, Mo) Mirror	15	40	67	0,62	CDM _B (EP10)	n/a
	S7	VIS Spectroscopy	Limiters	4	-		18,26	40	56	3,41	CDM _C (EP1 & EP5)	n/a
[3 - 5] µm	S8	Thermography	Divertor	8	-		18,33	300	73	0,28	CDM _A (EP9 & EP12) and CDM_C (EP1 & EP5)	n/a
	S9	Thermography	Limiters	4	-		18,1	300	55	3,97		n/a
[780nm-2.5µm]	S10	ECE for IR Intensity[1]	Core	2	-	(SS) Mirror	45	78	100	**	CDM _A (EP9 & EP12)	n/a
[0.01nm - 5µm]	S11	Radiation Power	Core	13	8	(Au + Kapton or Pt + SiN) Bolometer[2] [11,12]	8*	4,3	313	**	CDM _A (EP9 & EP12)	CDM _A (VP9 & VP12)
	S12	Radiation Power	Edge	8	16		11	3,1	62	1,39		
	S13	Radiation Power	X-Point	-	4		8*	4,3	313	**	n/a	
	S14	Radiation Power	Divertor	12	-		14	2,5	69	0,51	CDM _B (EP10)	n/a

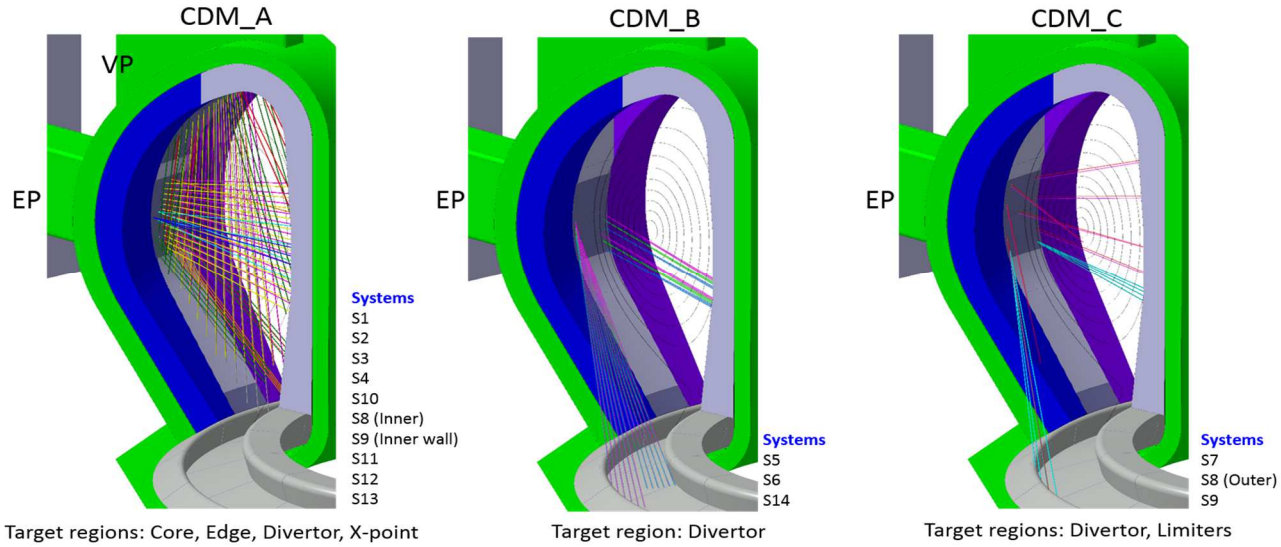

Figure 3: Sightlines configuration on compound diagnostic modules A, B, C and system integration.

Systems S1 and S2 based on X-ray measurements, are mainly influenced by the changes in the transmission (T). Filter foils based on Be are still popular, even though, thin beryllium foils are of limited supply and the toxicity of beryllium poses a health risk. However, there have been some efforts to use graphenic carbon (GC), directed to exploiting its properties as a superior window material, showing high transmission in the low energy region (0.1-3 keV) [13]. FOC locations for this group are expected to stay at L ≥7.2 m of distance from openings, ensuring a safe location for crystals and detectors; where low transmission losses are expected with the use of (D_2) as work gas, and the eventual deposition of few nanometers of W or erosion on filter foils will have a negligible impact on the transmission [14].

Systems from S3 to S10 based on the use of mirrors, are mainly influenced by the changes in the reflectance, as unfavorable consequence of environmental conditions that may entail changes in the surface/coating, such as erosion, particle deposition, and oxidation or mechanical stress. Although metallic and ceramic coating compounds remain the main candidates used for mirror, they are a long way from demonstrating high thermomechanical and material stability in harsh environments [15].

In particular, on systems from S3 to S5 based on VUV measurements, significant reflection can only be achieved at small values of grazing angle; thus it is fair to say that mirrors in VUV range are more sensitive to damages, hence pure metallic mirrors (e.g., Au, Pt) are highly recommended to this applications [7]. Unfortunately, mechanical limits restrain grazing angles lower than δ≤13° at the EP (S4 and S5), limiting the reflectance in the wavelength range from 6 to 10 nm, and the spectra lines measurement for W; as planned in the proposal VUV spectrometer system for DEMO [2]. Nevertheless, this measurement is still applicable to EP-S3 and VP's.

Systems from S6 to S10 based on VIS and IR measurements are also vulnerable to changes in reflectance; however, maximum grazing angles estimated δ ≤ 45°, does not imply a great loss of reflectance; for instance, assuming a Mo mirror, its reflectance in normal conditions is R > 0.6 in visible, from 400 to 700 nm and R > 0.9 in IR, from 3 to 5 μm at δ = 45° [15]. In particular, ECE measurements are less sensitive to first-mirror degradation because of the long wavelength (near IR), allowing the use of stainless steel (SS) mirrors with modest optical quality [16].

Systems from S11 to S14 based on total radiation measurements (X-ray + VUV + VIS and IR) by means of bolometers, are constrained by all the aspects already mentioned above, with previous observations remaining valid too; nevertheless, the installation of mirrors to provide neutron shielding is under consideration. In general, in all sightline configurations, FOC's shows a ratio $(L/\rho)_{min} > (L/\rho)$ in accordance with the criteria previously mentioned in 2, and an expected surface roughness h_f after 5 fpy of operation equal to $h_f < h_{max}$ [6], ensuring a high specular reflection throughout their lifetime.

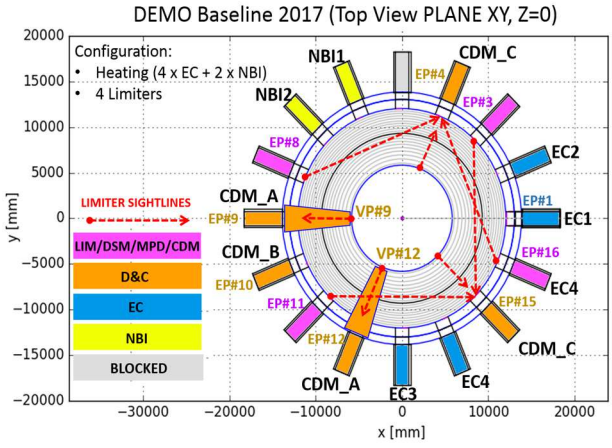

Figure 4: CDM distribution on DEMO proposal. Abbreviations: EC = Electron Cyclotron System, NBI = Neutral Beam Injection, CDM = Compound Diagnostic Module, LIM = Limiter, DMS = Disruption Mitigation System, MPD = Multipurpose Deployer.

4. Conclusion

Conceptual studies have been carried out on 14 D&C systems for spectroscopy and radiation measurements with subsequent integration into the DEMO baseline 2017 model, for a total of 310 optical sightlines, including redundancy. Diagnostics methods have been evaluated as function of their signal wavelength, target region, FOC's feasible locations and geometrical limits, at EP's and VP's. Main parameters such as transmission and reflectance, have been discussed, to identify the critical sightline configuration of every system and determine their feasibility. To conclude, an integration concept of these D&C systems and their distribution on 5 sectors of DEMO is proposed, based in 3 types of DCM, see Figure 3. A new, simplified and more integrated list of sightlines and channels for spectroscopy and radiation measurement for plasma control on DEMO is proposed in [17], nevertheless, the conclusions presented in this work are still valid for the development of a DEMO D&C conceptual design.

Acknowledgments

This work has been carried out within the framework of the EUROfusion Consortium and has received funding from the Euratom research and training programme 2014-2018 under grant agreement No 633053. The views and opinions expressed herein do not necessarily reflect those of the European Commission.

References

[1] F. Romanelli, "Fusion Electricity - A roadmap to the realisation of fusion energy," 2013. [Online]. Available: https://www.euro-fusion.org/wpcms/wp-content/uploads/2013/01/JG12.356-web.pdf.

[2] W. Biel et al., Internal document. Final report EFDA_D_2N4TFS (2016)

[3] W. Biel et al., Fus. Eng. Des. 96–97 (2015) 8–15

[4] G. Federici et al., Fus. Eng. Des. 89, (2014) 882-889

[5] R. Ambrosino et al., DEMO baseline 2017: Reference flat-top equilibria, EFDA_D_2MUW9R v1.0

[6] N. Pinel, et al. Progress In Electromagnetics Research B, Vol. 19, 41–63, 2010

[7] F.P. Orsitto et al., Nucl. Fusion 56 026009, (2016)

[8] M.Z. Tokar, Nucl. Fusion 58, (2018) 096002,

[9] E.M. Hollmann et al., Nucl. Fusion 53 083004 (2013)

[10] G. Taylor et al., Fus. Sci. Tech. 55,64 (2015)

[11] H. Meister et al., Fus. Eng. Des. 120, 21–26 (2017)

[12] L. Giannone et al., Plasma Phys. Cont. Fus. 47, 2123, (2005).

[13] S. Huebner et al., IEEE Trans Nucl. Science, vol. 62, no. 2, pp. 588-593, (April 2015)

[14] Henke, B.L., et al., Atomic Data and Nuclear Data Tables, vol. 54, no. 2, pp.181-342, (July 1993)

[15] A. Pereira et al., Steam and humidity test report, F4E_FPA-407-SG 07, DC-4T006-D001

[16] V. Udintsev et al., Internal ITER document. DDD Diag. Elec. Cycl. Emss. IDM_679HW9 (2012)

[17] W. Biel et al., Proc. 30th SOFT conference (2018)